# Original Article Mic60/Mitofilin inhibitor, Miclxin, induces rat H9C2 cardiomyoblast death by inhibiting the removal of damaged mitochondria

Muhammad S Khan<sup>1</sup>, Somayyeh Nasiripour<sup>1</sup>, Michele Oyarzabal<sup>1</sup>, Swati Banerjee<sup>1</sup>, Kumar Sharma<sup>2</sup>, Manzoor A Bhat<sup>1</sup>, Jean C Bopassa<sup>1</sup>

<sup>1</sup>Department of Cellular and Integrative Physiology, School of Medicine, University of Texas Health Science Center at San Antonio, San Antonio, TX 78229, USA; <sup>2</sup>Center for Precision Medicine, School of Medicine, University of Texas Health Science Center at San Antonio, San Antonio, TX 78229, USA

Received November 1, 2024; Accepted July 5, 2025; Epub September 15, 2025; Published September 30, 2025

Abstract: Mitochondrial dysfunction is a hallmark of various pathologic conditions, including ischemia/reperfusion injury, stroke, myocardial infarction, neurodegeneration and metabolic syndrome. As with all biological organelles, the function of mitochondria is tightly linked to their structure. The inner mitochondrial membrane is a highly regulated membrane with a large surface area that hosts the electron transport chain machinery, generates the membrane potential necessary for ATP generation, and forms the signature cristae folds of mitochondria. The mitochondrial inner membrane protein (Mitofilin/Mic60) is part of a large complex that constitutes the mitochondrial inner membrane organizing system, which is critical in maintaining mitochondrial architecture and function. Recent evidence has shown that Mic60/Mitofilin elimination during reperfusion determines the extent of myocardial infarct size after ischemia/reperfusion. Here, we investigated the effects and mechanisms of action of Miclxin, a novel Mic60/Mitofilin inhibitor using H9c2 cardiomyoblasts. Cultured rat H9c2 cardiomyoblasts were incubated with 0. 5, 10, or 20 µM of Miclxin. Cell viability was determined using 3-(4, 5-dimethylthiazol-2-yl)-2, 5-diphenyltetrazolium bromide (MTT) assays, and cell death was determined by flow cytometry using propidium iodide dye. Mitochondrial membrane potential was measured using MitoTracker Red CMXROS assay kits, and mitophagy in mitochondria was detected using Mitophagy Detection Kits. Mitochondrial morphology was assessed using electron microscopy, and proteins were measured by Western blot analyses and immunofluorescence staining. After 24 hours of treatment, Miclxin decreased cell viability in a dose-dependent manner and reduced the number of viable cells measured with MTT assays. This effect was associated with pronounced reduction of Mic60 protein levels measured by Western blots and immunocytochemistry. Miclxin's reduction of cell viability was related to its inhibition of mitochondrial elimination by mitophagy. Our findings suggest that Miclxin decreases levels of Mic60, and thereby reduces cell viability by increasing structural damage and dysfunction in mitochondria via impairment of mitophagy.

Keywords: Mic60/Mitofilin protein, Miclxin, mitophagy, H9C2 rat cardiomyomyoblasts, mitochondria, cell viability

#### Introduction

Mitochondria are essential organelles whose function is crucial to homeostasis, energy generation, and cellular fate. Mitochondria are recognized as the "powerhouse" of eukaryotic cells, especially in those that require highenergy demand such as cardiomyocytes [1]. Therefore, mitochondrial dysfunction is a hallmark in a variety of disease conditions, including in ischemia/reperfusion (I/R) injury, stroke, and myocardial infarction, metabolic syndrome, neurodegeneration, and aging [2-5]. In the

human heart, mitochondria occupy around 30% of the total volume of the cardiomyocytes [6], and these organelles supply, through oxidative phosphorylation (OXPHOS), approximately 6 kg of adenosine triphosphate (ATP) per day [7], which is required to sustain cardiomyocyte function in the heart [4, 8]. In addition to their pivotal role in energy production, mitochondria also play an important role in cell signaling, reactive oxygen species (ROS) generation, and Ca<sup>2+</sup> buffering [9, 10]. In addition, mitochondria are the central hub of cellular metabolism providing metabolites for biosynthesis and produc-

ing ROS [11]. As with all biological organelles, the function of mitochondria is tightly linked with their structure. The mitochondrial inner membrane (IMM) has a unique composition of proteins [8] and phospholipids, whose interdependence is crucial for mitochondrial function. It is highly enriched in proteins specific to this membrane, the majority of which are encoded by the nuclear genome and imported from the cytosol [12]. The IMM is a highly regulated, large surface area membrane that hosts the electron transport chain (ETC) machinery, generates membrane potential necessary for ATP generation, and forms the signature folds of mitochondria, known as cristae.

Recent evidence has highlighted the importance of cristae morphology in mitochondrial function and cell survival, with a particular focus on the mitochondrial inner membrane organizing system (MINOS or MICOS) [13] in which Mic60 is the "core" of MICOS [14]. The MINOS or MICOS system is composed of many subunits, such as Mic60/Mitofilin, Mic10, coiled-coil-helix-coiled-coil-helix domain containing 3 (Mic19/CHCHD3), coiled-coil-helixcoiled-coil-helix domain containing 6 (Mic25/ CHCHD6), Mic13/Qil1, coiled-coil-helix-coiledcoil-helix domain containing 10 (Mic14/ CHCHD10), Mic23/ApoO, and apolipoprotein O like Mic27/ApoOL. Mic60 and Mic10 are considered the most critical components of MICOS. Mic60 is recognized as the "core" of MINOS and a critical transmembrane IMM protein whose downregulation, modification, or destruction results in mitochondrial dysfunction and cell death [15, 16]. This suggests a critical role of Mic60 in the mechanism of cell death, a major hallmark of many mammalian diseases such as neurodegenerative disease, stroke, and myocardial infarction [17]. We recently reported that after heart I/R injury, depletion of Mic60 impairs cardiac functional recovery, increases myocardial infarct size, and facilitates mitochondrial structural damage and dysfunction [18]. After acute renal I/R injury, we have shown that the receptor-interacting protein kinase 3 (RIP3) translocates into mitochondria to promote Mic60 degradation, which initiates an increase in kidney inflammation and injury [19]. Our group further revealed that Parkin interacts with Mic60 in response to Parkinson's disease stressor neurotoxicity. which leads to the degradation of Mic60, resulting in mitochondrial structural damage and dysfunction that is responsible for neuronal death by apoptosis [20].

The role of Mic60 in cell death has been abundantly studied using cell lines transfected with siRNA and Mic60-overexpressed plasmids [16, 20]. More recently, a drug, referred to as Miclxin, has been reported to inhibit Mic60 function [21]. In fact, using Miclxin-immobilized beads, Imoto's group identified Mic60 as a target protein of this compound. In that study, authors concluded that targeting Mic60 with Miclxin represents a potential strategy with which tumor cells can be killed through induction of severe mitochondrial damage in a mutant β-catenin-dependent manner. However, further studies determining the role and mechanisms of Miclxin in cell viability and death in normal cells (non-tumor cells) is still needed. In addition, whether Miclxin only induces inhibition of Mic60, as well as elimination still needs to be clarified, as Mic60 elimination is well known to induce cell death in several cell lines. In this study, we unveiled the effects of Miclxin in cell viability and death using cultured rat H9c2 cardiomyoblasts. We report that Miclxin induces H9c2 cardiomyoblast death by increasing elimination of Mic60 protein levels, which contributes to mitochondria structural damage and dysfunction through impaired mitochondria removal by mitophagy.

# Materials and methods

# Institutional approval

Protocols followed the Guide for the Care, and Use of Laboratory Animals (US Department of Health, NIH), and received UT Health Science Center at San Antonio Institutional Animal Care and Use Committee (IACUC) institutional approval. Animals were housed in the animal specific pathogen free facility at UTHSCSA main campus in cages with standard wood bedding and space for five mice or two rats. The animals had free access to food and drinking water and a 12-hour shift between light and darkness. The animals were selected randomly, and the data analysis was performed blindly.

### Cell culture

The rat H9c2 cardiomyoblast line was purchased from the American Type Culture

Table 1. List of antibodies used in this study

Antibody Target	Supplier	Catalog #	Concentration
Mitofilin/Mic60	Proteintech Group	10179-1-AP	1 µg/mL
LC3I/LC3II			1 µg/mL
p-p62			1 µg/mL
Pink1			1 µg/mL
Ubiquitin			1 µg/mL
VDAC1 and VDAC3			1 μg/mL
GAPDH			1 µg/ml
IRDye 800CW Goat anti-Rabbit	LI-COR	926-32211	0.1 μg/mL
IRDye 680RD Goat anti-Mouse	LI-COR	926-68070	0.1 μg/mL

Collection (ATCC no. CRL-1446), and the HEK 293 cell line was obtained from ATCC (no. CRL-3216). Cells were cultured in Dulbecco's modified Eagle's medium (DMEM; Invitrogen Life Technologies) supplemented with 10% fetal bovine serum (FBS; GIBCO-BRL, Grand Island, NY), 100 U/ml penicillin-streptomycin and grown in an atmosphere of 5%  $\rm CO_2$ -95% humidified air at 37°C. The culture medium was changed every second day. Cells were used between passage 4 and 7, at 70-80% confluence. The cells were selected randomly, and the data analysis was performed by a blind investigator.

# Treatment of cells with Miclxin

Rat H9c2 cardiomyoblasts were incubated for 24 hours in the presence of Miclxin (5, 10 20  $\mu$ M), or Vehicle (0.01% DMSO in media). Twenty-four hours post treatment; cells were trypsinized and collected for further applications.

# Cell viability

Cell viability was determined using the tetrazolium dye 3-(4, 5-dimethylthiazol-2-yl)-2, 5-diphenyltetrazolium bromide (MTT) assay by following standard protocols. Briefly, cells were cultured in a 96 well plate and treated with either Vehicle or Miclxin as described above. At the end of the treatment, cells were placed in 50  $\mu L$  of serum-free media supplemented with 50  $\mu L$  of MTT solution into each well for 3 h incubation. After that, 150  $\mu L$  of DMSO was added into each well before absorbance was read at 590 nm.

# Western blot analysis

Equal amounts of the whole lysate protein were loaded in each well of 4-20% Tris-glycine gels

(Bio-Rad) as recently described in [19]. After electrophoresis for 90 min at 125 V of constant voltage, the gel was blotted onto a nitrocellulose membrane by electrophoretic transfer at 70 V of constant voltage for 1-2 h. The membrane was washed, blocked with 5% blocking solution, and probed with various primary antibodies: anti-Mic60 (Abcam, catalog no. ab110329), and anti-GAPDH (CST, catalog no. 2118S) at 4°C overnight. The immunoreactive bands were visualized using secondary Li-Cor antibodies (LI-COR Biotechnologies, Lincoln, NE): Ire 800CW goat anti-rabbit antibody, (catalog no. 926-32211) and IRDye 680RD goat anti-mouse antibody, (catalog no. 926-68070).

### Antibodies and reagents

All materials were purchased from Sigma-Aldrich, unless otherwise stated. Studies utilized antibodies against the targets listed in **Table 1**.

# Mitochondrial membrane potential measurement

Mitochondrial membrane potential measurement (ΔΨm) was assessed using MitoTracker Red CMXROS assay kit (ThermoFisher Scientific, catalog no. M7512) by fluorescent microscopy according to manufacturer's protocol. MitoTracker red dye is a red-fluorescent dye that stains mitochondria in live cells and its accumulation is dependent upon membrane potential. H9c2 myoblasts were plated in sixwell plates for MitoTracker Red assay or on coverslips for labeling and allowed to reach 70-80% confluence, after which cells were treated with vehicle, or Miclxin for 24 h. Live cells were harvested and incubated with MitoTracker Red (150 nM) for 1 h at 37°C. Carbonyl cyanide m-chlorophenylhydrazone (CCCP) was used as

a control. Mitochondrial membrane potential was qualitatively assessed in normal and Miclxin-treated rat myoblasts using JC-1 dye (Cayman, 15003) [18, 22]. After 24 h transfection, media was carefully removed from twentyfour well plates and cells were washed twice with PBS, 0.5 ml of DMEM containing FBS. Cells were resuspended in DMEM containing FBS, stained by adding JC-1 (10 µg/ml) and cultured for 30 min at 37°C with continuous gently shaking. At the end of the incubation, the media was removed, and cells were washed twice with normal PBS. To image the cells, 0.5 ml of DMEM containing FBS was added to each well and images were taken with fluorescence microscopy.

### Immunofluorescence staining

Cells were cultured on coverslips and treated as described above. After treatment, cells were fixed with 4% paraformaldehyde for 15 min and permeabilized with 0.25% Triton X-100. After blocking in 3% BSA for 30 min. slides were incubated with the primary antibody diluted in 1% BSA for overnight. Coverslips were incubated with primary antibodies for Mic60 antibody (Proteintech Cat# 10179-1-AP, RRID:AB\_2127193), followed by secondary antibodies Alexa Fluor 488 Goat anti-rabbit (Abcam Cat# ab150077, RRID:AB\_2630356) and Goat anti-mouse (Abcam Cat# ab150113, RRID:AB\_2576208). Images were taken on a Zeiss Axiovert 200M inverted motorized fluorescence microscope (Carl Zeiss Microscope, Jena, Germany).

# Detection of mitophagy

Mitophagy in mitochondria was detected by use of a Mitophagy Detection Kit according to the manufacturer (Dojindo Molecular Technology, Rockville, MD, USA) as described in [23]. This kit is composed of Mtphagy Dye, reagent for detection of mitophagy, and Lyso Dye, reagent for staining of lysosomes allowing accurate quantification of the damaged mitochondria fusing to the lysosomes. The signal was detected in cultured H9c2 cardiomyomyoblasts using confocal microscopy analysis at the following wavelengths: Mtphagy Dye: 561 nm (Ex) and 650 nm (Em); Lyso Dye: 488 nm (Ex) and 550 nm (Em).

## Transmission electron microscopy

To analyze mitochondrial morphology in normal and I/R mice hearts, samples were fixed in a phosphate buffered solution of 4% formaldehyde with 1% glutaraldehyde, and stored at 4°C overnight as described in [23]. Tissue sections were washed with PBS, post-fixed in 2% (wt/ vol) osmium tetroxide for 2 h at room temperature, and dehydrated in a graded alcohol series before being embedded in Eponate 12 medium. The blocks were cured at 60°C for 48 h. and 70 nm sections were cut using an ultramicrotome, mounted on Formvar-coated grids and double-stained with uranyl acetate and lead citrate. The resulting samples were analyzed and imaged using a JEOL 1230 transmission electron microscope. Mitochondria were classified as 'damaged' if they had more than 50% disorganized/destroyed cristae structure. Mitochondrial area was calculated using ImageJ software.

# Flow cytometry analysis of cell death

Cell death was determined using Propidium iodide (BD PharMingen, catalog no. 556547) according to the manufacturer's instructions. Briefly, the harvested cells were washed twice in PBS and resuspended in 500 µl binding buffer. The cells were treated with 5 µl propidium iodide and immediately analyzed using a BD LSR II flow cytometer (BD Biosciences, San Jose, CA). Propidium iodide (PI) is a membrane-impermeable fluorescent dye that stains DNA and cells used to label dead cells.

#### Statistical analysis

Data presented in bar graphs are expressed as means, and error bars are the standard errors of the mean ( $\pm$  SD) for a minimum of three independent trials ( $n \ge 3$ ). Comparisons were conducted using the Student's t-test and one-way ANOVA with post-hoc Dunnett's or Tukey's corrections for multiple comparisons, where appropriate, using Prism 8 (Graphpad Software). A difference of P<0.05 was considered to be statistically significant.

#### Results

Miclxin induces Mic60 elimination

**Figure 1A** shows that Miclxin reduced levels of Mic60 in a concentration-dependent fashion

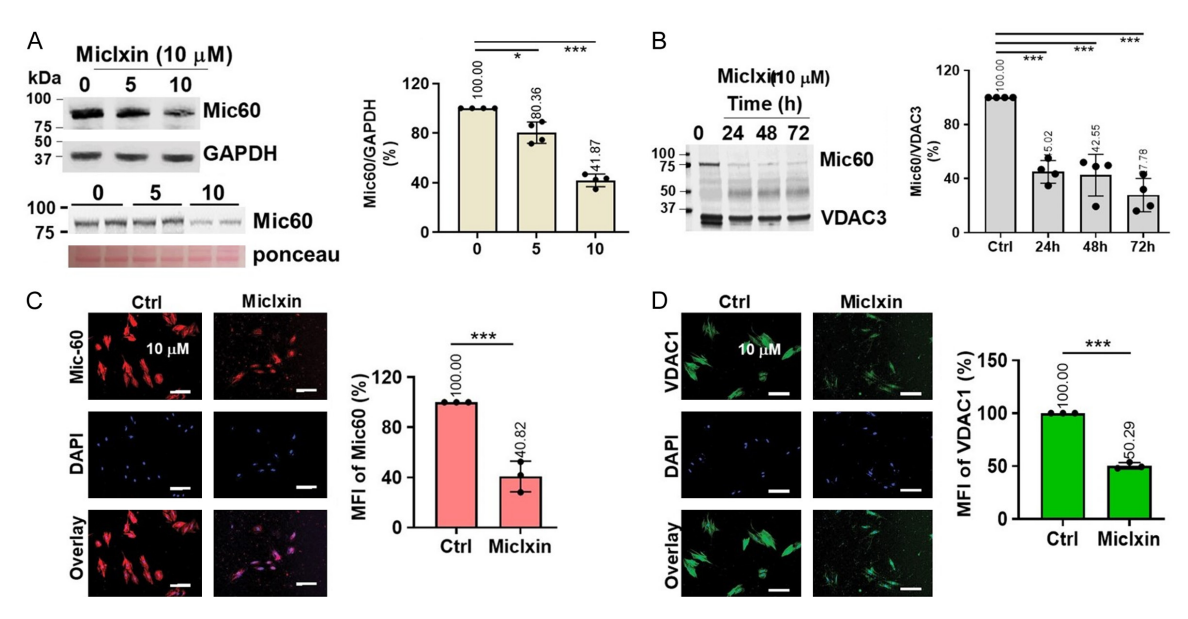


Figure 1. MicIxin treatment reduces Mic60 protein levels in a time and concentration-dependent manners. (A) Immunoblot and graph show a time (24, 48, and 72 h), and concentration-dependent (MicIxin 5, and 10 μM) decrease in Mic60 protein levels compared to normal cells (MicIxin 0 μM). Values are expressed as mean  $\pm$  S.D., n = 4/group. Data were analyzed with One-Way ANOVA; with \*P<0.05, and \*\*\*P<0.001 vs vehicle (MicIxin 0 μM). (B) Immunoblots and graph show a time-dependent (24, 48, and 72 h) decrease in Mic60 levels in MicIxin-treated cells (MicIxin, 10 μM) compared to normal cells (MicIxin 0 μM). Values are expressed as mean  $\pm$  S.D., n = 4/group. Data were analyzed with One-Way ANOVA; with \*\*\*P<0.01 vs vehicle (MicIxin 0 μM). (C) Images of cells treated with Mic 60, and VDAC1 (D) antibodies, DAPI, and the overlay of both signals. Graphs show a decrease in Mic60 and VDAC1 fluorescence intensity in MicIxin-treated cells (MicIxin 10 μM) compared to normal cells. Values are as mean  $\pm$  S.D., n = 3/group. Data were analyzed with unpaired t-test with \*\*\*P<0.001 vs vehicle (MicIxin 0 μM).

compared to untreated cells. Compared to untreated cells, levels of Mic60 were reduced to 80.36±7% in cells treated with Miclxin (5 μM), and to 45.02%±7% in cells treated with Miclxin (10  $\mu$ M) (n = 4 experiments/group). Furthermore, these reductions were timedependent. Compared to untreated cells levels of Mic60 were reduced to 45.01±7% after 24 hr treatment with Miclxin, 42.54±13% after 48 hr treatment with Miclxin, and 27.78±10% after 72 hr treatment with Miclxin (n = 4 experiments/group) (Figure 1B). These results indicate that Miclxin inhibits Mic60 function by increasing its elimination in cultured H9c2 cardiomyoblasts. We also measured levels of Mic60 and VDAC1 by fluorescence microscopy after treatment with Miclxin (10 µM) in H9c2 cardiomyoblasts. Miclxin at that dose decreased levels of both Mic60 and compared to untreated cells (Figure 1C and 1D). Compared to untreated cells, levels of Mic60 and decreased to 39%±8% and 50%±3%, respectively (n = 3 experiments/group) (Figure 1C and 1D).

Miclxin-induced Mic60 loss decreases cell viability and increases cell death

Compared to untreated cells, Miclxin reduced H9c2 myoblast viability in a concentrationdependent manner (Figure 2A). H9c2 myoblasts were reduced to 96.52%±7% in Miclxin 5  $\mu$ M, 65.24±3% in Miclxin 10  $\mu$ M, and 27.53±2% in Miclxin 20  $\mu$ M (n = 4 experiments/group) (Figure 2B). We also found a time-dependent decrease in cell viability in Miclxin-treated cells compared to untreated cells. H9c2 myoblast viability was reduced to 64.41%±3% in Miclxin after 24 h, 43.25±6% in Miclxin after 48 h, and  $13.33\%\pm7\%$  in Miclxin after 72 h (n = 6 experiments/group (Figure 2C). Flow cytometry analyses showed that Miclxin (10 µM) increased H9c2 cardiomyoblast death compared to untreated cells (Figure 2D). H9c2 myoblast death was increased to 149.42%±2% at that dose (n = 3 experiments/group) (Figure 2D). Taken together, these results indicate that Miclxin treatment reduced rat H9c2 cardiomyoblast viability and increased cell death.

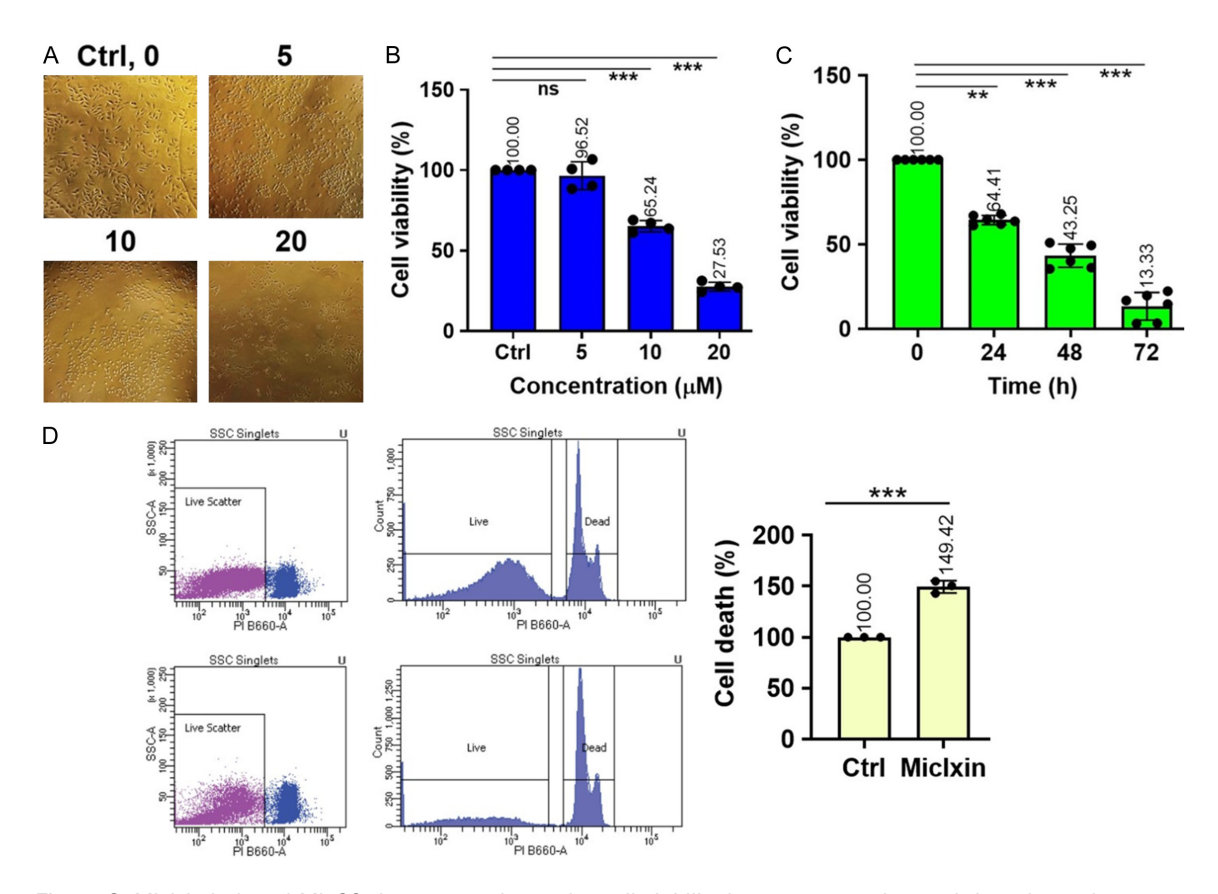


Figure 2. Miclxin-induced Mic60 decrease reduces the cell viability in a concentration and time dependent manners. A. Image of H9c2 cells in function of Miclxin concentration. Values are expressed as mean  $\pm$  S.D., n = 6/group. Data were analyzed with One-Way ANOVA; with \*\*P<0.01, and \*\*\*P<0.001 vs vehicle (Miclxin 0  $\mu$ M). B. graph shows a concentration-dependent (Miclxin 5, 10 and 20  $\mu$ M) decrease in cell viability compared to normal cells (Miclxin 0  $\mu$ M). C. Graph shows a time-dependent (24, 48, and 72 h) decrease in cell viability in Miclxin-treated cells (Miclxin, 10  $\mu$ M) compared to normal cells (Miclxin 0  $\mu$ M). Values are expressed as mean  $\pm$  S.D., n = 6/group. Data were analyzed with One-Way ANOVA; with \*\*P<0.01, and \*\*\*P<0.001 vs vehicle (Miclxin 0  $\mu$ M). D. Flow cytometry analysis of cell death with Propidium iodide shows an increase in the rate of cell death and reduction of the number of live cells in Miclxin (10  $\mu$ M) treated group compared to untreated group. Values are expressed as mean  $\pm$  S.D., n = 3/group. Data were analyzed with unpaired t-test; with \*\*\*P<0.001 vs vehicle (Miclxin 0  $\mu$ M).

Miclxin reduces cell viability by promoting mitochondrial dysfunction

To assess the mechanism responsible for Miclxin-induced reduction of cell viability, we determined whether MMP was impacted by Miclxin treatment. Numbers of MitoTracker redpositive cells decreased as Miclxin concentrations increased (Figure 3).

We also assessed MMP using JC-1 dye. Compared with untreated cells, ratios of green (Aggregate)/red (Monomer) fluorescence intensity increased as the concentrations of Miclxin increased (**Figure 4**). Ratios of green/red fluorescence intensity increased to  $784.15\pm84$  (arbitrary units) in cells treated with Miclxin at 5  $\mu$ M, and to  $2184.48\pm156$  (arbitrary units) in

cells treated with 10  $\mu$ M Miclxin (n = 3 experiments/group). This result suggests that Miclxintreated mitochondria are more uncoupled than untreated mitochondria. Together, these results indicate that treatment with Miclxin induces dissipation of MMP in H9c2 myoblasts, which induces mitochondrial dysfunction.

Miclxin induces mitochondrial dysfunction by altering mitophagy

Next, we studied whether Miclxin's actions on mitochondria via Mic60 elimination are due to altered removal of damaged mitochondria by mitophagy. We treated H9c2 cells with Miclxin at 0, 5, and 10  $\mu$ M for 24 hours; mitophagy was evaluated based on the number of engulfed mitochondria. Using electron microscopy, we

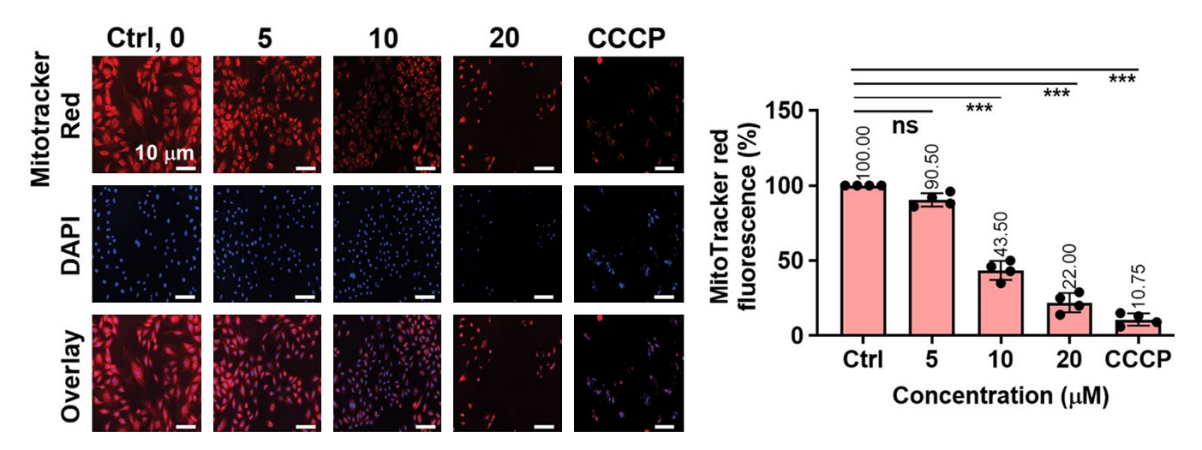


Figure 3. Mitochondria from cells treated with Miclxin are more uncoupled compared to normal cell mitochondria. Top: Images of cells treated with MitoTracker red dye, DAPI, and the overlay of both signals. Bottom: graph shows a decrease in the fluorescence of MitoTracker red dye in Miclxin-treated cells (Miclxin 5, 10 and 20  $\mu$ M) compared to normal cells. Values are as mean  $\pm$  S.D., n = 4/group. Data were analyzed with One-Way ANOVA; with \*\*P<0.01, and \*\*\*P<0.001 vs vehicle (Miclxin 0  $\mu$ M).

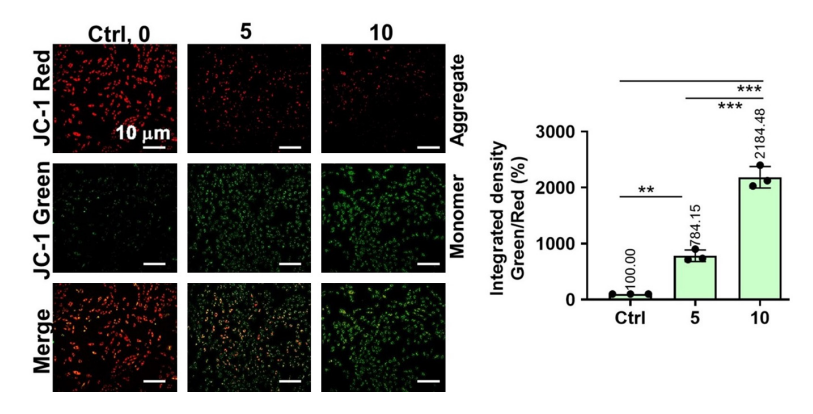


Figure 4. Mitochondria from cells treated with Miclxin are more uncoupled compared to normal cell mitochondria. Images of cells (top) and graph (bottom) show an increase in the green (monomer)/red (aggregation) fluorescence ratio of JC-1 dye in Miclxin-treated cells (Miclxin 5, and 10  $\mu$ M) mitochondria compared to normal cells mitochondria. Values are expressed as mean  $\pm$  S.D., n = 3/group. Data were analyzed with One-Way ANOVA; with \*\*\*P<0.001 vs vehicle (Miclxin 0  $\mu$ M).

observed that mitochondrial structural integrity was preserved in untreated cells compared to Miclxin-treated cells. Although the number of mitochondria was not significantly different between groups, mito-phagosomes were more abundant after Miclxin treatment versus untreated cells (Figure 5). Numbers of engulfed mitochondria were markedly increased in treated cells compared to untreated cells, suggesting altered removal of the damaged mitochondria.

To determine how Miclxin alters mitophagy in H9c2 cultured cells, we studied how the PINK1 pathway, which is involved in mitophagy via

autophagy adaptors [24], affects the action of Miclxin. Using Western blot analysis, PINK1 protein levels were decreased in Miclxin-treated cells compared to untreated cells (Figure 6). We also found that Miclxin treatment increased ratios of the microtubule-associated 1A/1B-light chain 3 (LC3) LC3II/LC3I and decreased p-protein p62/Sequestosome 1 (p62) and total ubiquitin levels compared with untreated cells (Figure 6). These results suggest that Miclxin alters mitophagy by deactivation of the PINK1 pathway.

To confirm this observation, the flux of mitophagy was evaluated using mitodye and lysodye assays. Mitochondrial autophagosomes fuse with lysosomes during mitophagy, and the fluorescence intensity of Mtphagy dye increases. Alteration of mitophagy is associated with increased lysodye uptake, measuring mitochondria engulfed in autophagosomes. As shown in Figure 7, accumulation of autophagosomes was markedly increased in cells treated with 10  $\mu$ M Miclxin, similar to cells treated with CCCP versus untreated cells. Together, these data support the hypothesis that Miclxin action via Mic60 elimination involves altered mitophagy, resulting in accumulation of damaged mito-

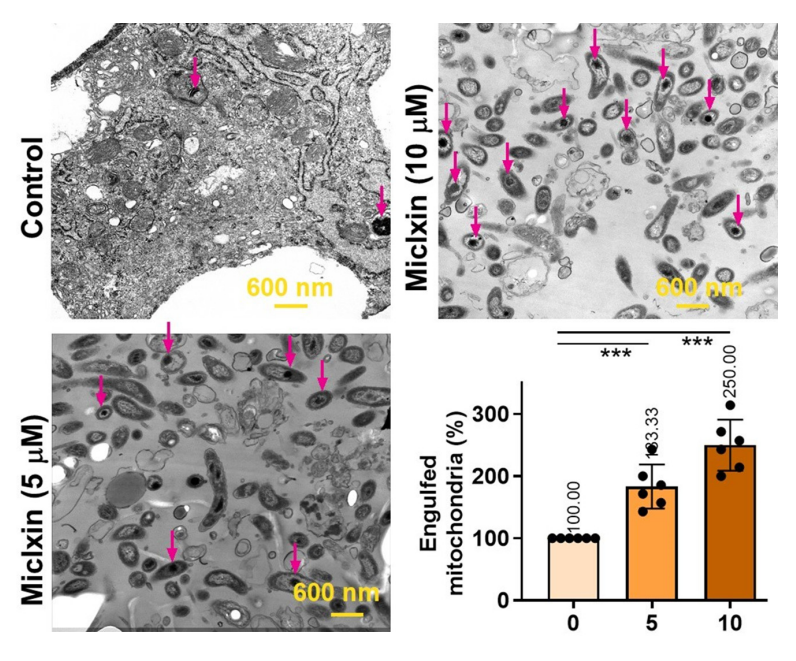


Figure 5. Miclxin treatment increases the number of engulfed mitochondrial. Electron microscopy images of mitochondria in H9c2 cells (magnification  $25000\times$ ) from Miclxin-treated cells and normal cells (control) showing a better mitochondrial structure integrity in untreated mitochondria in which mitochondrial cristae are intact versus Miclxin-treated mitochondria treated in which mitochondrial cristae morphology is drastically disrupted and damaged. Note that in Miclxin-treated cells the number of mito-phagosomes is drastically increased compared to untreated cells suggesting alteration of the removal of damaged mitochondria. Values are as mean  $\pm$  S.D, n = 6/group. Data were analyzed with One-Way ANOVA; with \*\*P<0.01, and \*\*\*P<0.001 vs vehicle (Miclxin 0  $\mu$ M).

chondria that is responsible for mitochondrial dysfunction.

# Discussion

Here, we report that Miclxin treatment decreased cultured H9c2 cardiomyoblast viability by enhancing Mic60 elimination. This effect was associated with increased alterations in removal of damaged mitochondria by mitophagy.

Mitochondria play a crucial role in cardiac cells, including (but not limited to) energy production, calcium homeostasis, and regulation of cell death [25, 26]. The structure of mitochondria and the protein composition of its inner membrane have received increasing importance in determining the function of mitochondria in health and pathophysiology [27, 28]. Mic60 is now recognized as the core unit of the MINOS complex - the critical organizer of mitochondrial cristae morphology, and thus essential for normal mitochondrial function [29].

Previously, our group demonstrated that Mic60 knockdown in H9c2 cardiomyoblasts by siRNA induced mitochondrial structural damage, leading to increased cell apoptosis via an Apoptosis-Inducing Factor (AIF)-Poly (ADPribose) polymerase (PARP) pathway [16]. More recently, we reported that knockdown of Mic60 in mice increases mitochondrial structural damage and dysfunction. These changes cause critical failures of mitochondria to regulate Ca2+ homeostasis, leading to increased mitochondrial sensitivity to Ca2+ overload favoring mPTP opening, and subsequently causes cardiomyocyte death. Furthermore, in an I/R model, we found that loss of Mic60 during early reperfusion [18] induces dysregulation of members of the mitochondrial carrier family (SLC25). These carriers promote an increase in generation of reactive oxygen species that facilitates the re-

lease of mitochondrial DNA into the cytosol. This activates the signaling pathway that augments nuclear transcription of pro-inflammatory cytokines that subsequently exacerbate I/R injury.

Recently, Miclxin was identified as an inhibitor of Mic60 that induces apoptosis through mitochondrial stress in B-catenin mutant tumor cells [21]. Mic60 dysfunction caused by Miclxin induced a mitochondrial stress response in a mutant β-catenin-dependent manner. When we treated different concentrations of Miclxin in cultured H9c2 cardiomyoblasts, we found that Miclxin induced a concentration-dependent reduction of Mic60 protein levels (Figure 1). This observation, similar to those previously reported with Mic60 knockdown in H9c2 and HEK 293 cells transfected with Mic60siRNA [16], indicates that Miclxin's mechanism of action includes dysfunction of Mic60 via its elimination. Concomitantly, Miclxin reduced cell viability time in a concentration-dependent manner (Figure 2B, 2C) and increased cell

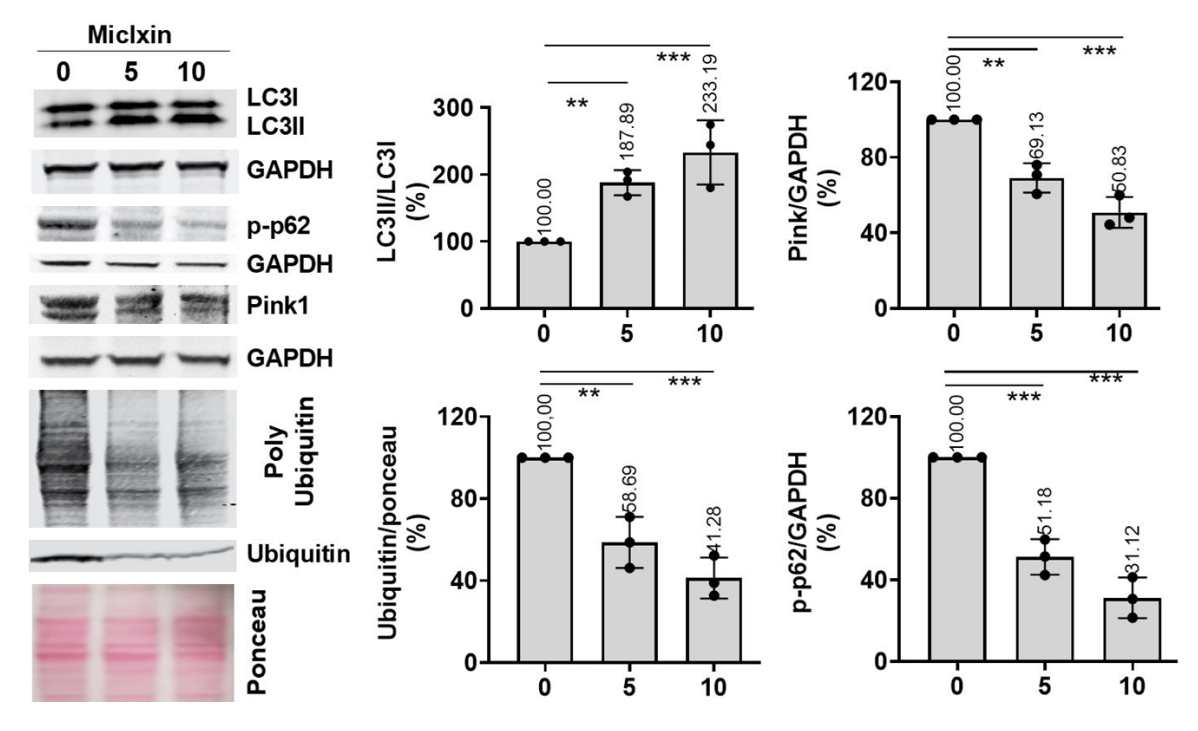


Figure 6. Miclxin treatment alters mitophagy via the PINK1 mechanism. In the whole-cell lysate, Miclxin treatment (5 and 10  $\mu$ M) decreased the protein levels of p62, ubiquitin and PINK1 expression and increased the LC3II/LC3I ratio compared to control (Miclxin, 0  $\mu$ M). Values are expressed as mean  $\pm$  S.D., n = 3/group. Data were analyzed with One-Way ANOVA; with \*P<0.05, and \*\*P<0.01 vs vehicle (Miclxin 0  $\mu$ M).

death (Figure 2D), suggesting that Miclxin induces cytotoxic effects by reducing Mic60. These effects were associated with altered removal of damaged mitochondria by mitophagy. Furthermore, Miclxin treatment reduced mitochondrial membrane potential in a concentration-dependent manner (Figures 3 and 4). This finding supports the conclusion that dysregulation of Mic60 by Miclxin contributes to mitochondrial depolarization, similar to CCCP, a mitochondrial uncoupler [21]. Supporting this concept, Miclxin treatment reduced VDAC1 protein levels similar to its effects on Mic60 (Figure 1).

Decreased mitochondrial membrane potential triggers removal of dysfunctional mitochondria by mitophagy via autophagy adaptors [30]. We thus examined whether Miclxin induces mitochondrial depolarization by changing mitophagy, ultimately exacerbating mitochondrial stress and accumulation of damaged and dysfunctional mitochondria. We found that Miclxin decreased Pink1, phosphorylation of P62, and mitochondrial protein ubiquitination, and was

associated with an increased LC3II/LC3I ratio (Figure 6). Accumulation of autophagosomes was markedly increased in Miclxin-treated cells compared to untreated cells (Figure 7). These results suggest that altered mitophagy is part of Miclxin's mechanism of action. Since Miclxin initiates mitochondrial depolarization, which promotes sequestration of mitochondria into autophagosomes [31], our results suggest that Miclxin alters removal of damaged mitochondria by inhibiting mitophagy dependent on the PINK1 pathway.

## Conclusions

We report that the Miclxin treatment in H9c2 cardiomyoblasts increases Mic60 elimination and thereby increases mitochondrial structural damage, which results in critical depolarization of mitochondria. We propose for the first time that Miclxin-induced altered removal of damaged mitochondria by mitophagy contributes to mitochondrial dysfunction that is responsible for reduced cell viability and increased cell death. The overall mechanism is represented in Figure 8.

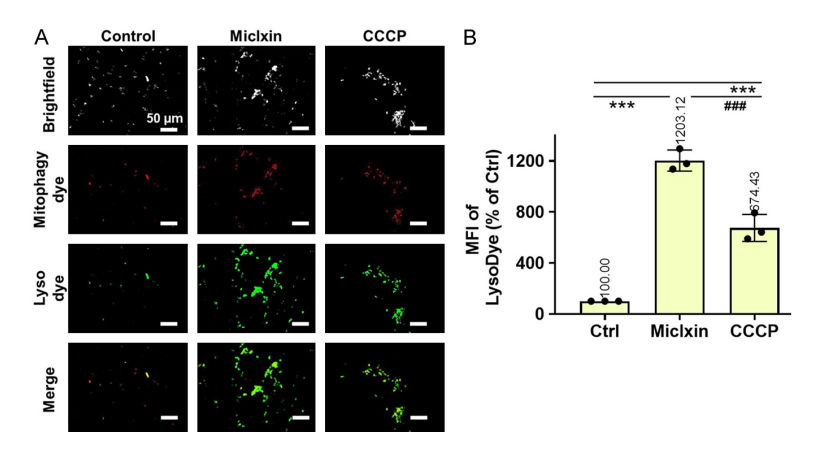


Figure 7. Miclxin treatment increases accumulation of autophagosome. A. Fluorescence intensity of brigthfield and mitochondrial Mtphagy Dye (red) and Lyso Dye (green) in H9c2 cardiomyoblasts; B. Quantitative analyses of average fluorescence intensity of mitochondrial Lyso Dye in cells. Values are as mean  $\pm$  S.D., n = 3/group. Data were analyzed with One-Way ANOVA; with \*\*\*P<0.001, vs untreated (control) group (Miclxin 0  $\mu$ M), \*\*\*\*P<0.001 (Miclxin 10  $\mu$ M) vs CCCP group.

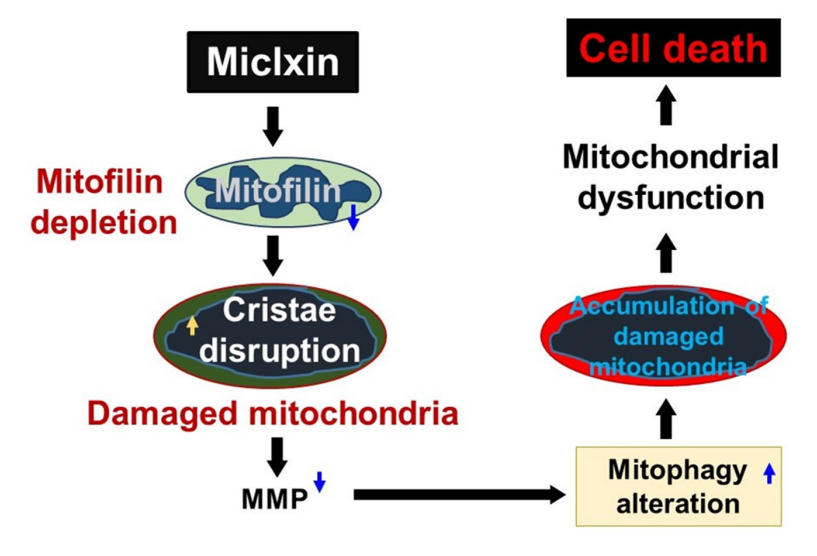


Figure 8. Scheme depicting the mechanism of Miclxin-induced reduction of H9c2 myoblast viability, which is associated with cell death. Miclxin treatment in H9c2 cardiomyoblasts increases Mic60 elimination, which induces mitochondrial structural damage resulting in critical depolarization of mitochondria. The resulted alteration of the removal of damaged mitochondria by mitophagy facilitates dysfunction of mitochondria that is responsible for decrease in cell viability and subsequently leading death.

# Limitations

We used only rat H9c2 cardiomyoblasts, so the effects we observed should be confirmed in another cell line. Also, *in vivo* studies investigating the effects of Miclxin are needed. Finally, while we report that Miclxin induces Mic60 reduction, that effect may be the consequence

of its initial inhibition. Further studies are needed to examine the effects of Miclxin in acute conditions.

# Acknowledgements

This work was supported by R01 HL138093 (JCB), T32 HL007446-41 (JCB), and R25 NS115552 (MAB).

# Disclosure of conflict of interest

None.

#### **Abbreviations**

Mic60, Inner mitochondrial membrane protein; ROS, reactive oxygen species; MICOS, mitochondrial contact site and cristae organizing system; MMP, mitochondrial membrane potential; CCCP, Carbonyl cyanide m-chlorophenylhydrazone; LC3, Microtubuleassociated protein 1A/1Blight chain 3; p62. The protein p62/Sequestosome 1; AIF, Apoptosis-Inducing Factor; PA-RP, Poly (ADP-ribose) polymerase; mtDNA, Mitochondrial DNA: SLC25A. Members of the mitochondrial carrier family (SLC25); ETC, electron transport chain; APOOL, cardiolipin-binding component of the MINOS protein complex; CHCHD, coiled-coil-helix-coiled-coil-helix domain; RIP3, receptor-interacting protein kinase 3; MTT, 3-(4, 5-dimethy-Ithiazol-2-yl)-2, 5-diphenyltet-

razolium bromide; GAPDH, Glyceraldehyde 3-phosphate dehydrogenase.

Address correspondence to: Dr. Jean C Bopassa, Department of Physiology, School of Medicine, The University of Texas Health San Antonio, 7703 Floyd Curl Dr., San Antonio, TX 78229, USA. Tel: 210-567-0429; E-mail: bopassa@uthscsa.edu

## References

- [1] Nan J, Zhu W, Rahman MS, Liu M, Li D, Su S, Zhang N, Hu X, Yu H, Gupta MP and Wang J. Molecular regulation of mitochondrial dynamics in cardiac disease. Biochim Biophys Acta Mol Cell Res 2017; 1864: 1260-1273.
- [2] Saleh MC, Wheeler MB and Chan CB. Uncoupling protein-2: evidence for its function as a metabolic regulator. Diabetologia 2002; 45: 174-187.
- [3] Christophe M and Nicolas S. Mitochondria: a target for neuroprotective interventions in cerebral ischemia-reperfusion. Curr Pharm Des 2006; 12: 739-757.
- [4] Li A, Gao M, Jiang W, Qin Y and Gong G. Mitochondrial dynamics in adult cardiomyocytes and heart diseases. Front Cell Dev Biol 2020; 8: 584800.
- [5] Bernardi P, Colonna R, Costantini P, Eriksson O, Fontaine E, Ichas F, Massari S, Nicolli A, Petronilli V and Scorrano L. The mitochondrial permeability transition. Biofactors 1998; 8: 273-281.
- [6] Ramaccini D, Montoya-Uribe V, Aan FJ, Modesti L, Potes Y, Wieckowski MR, Krga I, Glibetic M, Pinton P, Giorgi C and Matter ML. Mitochondrial function and dysfunction in dilated cardiomyopathy. Front Cell Dev Biol 2020; 8: 624216.
- [7] Bhullar SK and Dhalla NS. Status of mitochondrial oxidative phosphorylation during the development of heart failure. Antioxidants (Basel) 2023; 12: 1941.
- [8] Cao YP and Zheng M. Mitochondrial dynamics and inter-mitochondrial communication in the heart. Arch Biochem Biophys 2019; 663: 214-219.
- [9] Bopassa JC, Ferrera R, Gateau-Roesch O, Couture-Lepetit E and Ovize M. PI 3-kinase regulates the mitochondrial transition pore in controlled reperfusion and postconditioning. Cardiovasc Res 2006; 69: 178-185.
- [10] Gomez L, Thibault H, Gharib A, Dumont JM, Vuagniaux G, Scalfaro P, Derumeaux G and Ovize M. Inhibition of mitochondrial permeability transition improves functional recovery and reduces mortality following acute myocardial infarction in mice. Am J Physiol Heart Circ Physiol 2007; 293: H1654-H1661.
- [11] Spinelli JB and Haigis MC. The multifaceted contributions of mitochondria to cellular metabolism. Nat Cell Biol 2018; 20: 745-754.
- [12] Akbar M, Essa MM, Daradkeh G, Abdelmegeed MA, Choi Y, Mahmood L and Song BJ. Mitochondrial dysfunction and cell death in neurodegenerative diseases through nitroxidative stress. Brain Res 2016; 1637: 34-55.
- [13] Kozjak-Pavlovic V. The MICOS complex of human mitochondria. Cell Tissue Res 2017; 367: 83-93.

- [14] John GB, Shang Y, Li L, Renken C, Mannella CA, Selker JM, Rangell L, Bennett MJ and Zha J. The mitochondrial inner membrane protein Mitofilin controls cristae morphology. Mol Biol Cell 2005; 16: 1543-1554.
- [15] Li H, Ruan Y, Zhang K, Jian F, Hu C, Miao L, Gong L, Sun L, Zhang X, Chen S, Chen H, Liu D and Song Z. Mic60/Mitofilin determines MI-COS assembly essential for mitochondrial dynamics and mtDNA nucleoid organization. Cell Death Differ 2016; 23: 380-392.
- [16] Madungwe NB, Feng Y, Lie M, Tombo N, Liu L, Kaya F and Bopassa JC. Mitochondrial inner membrane protein (Mitofilin) knockdown induces cell death by apoptosis via an AIF-PARPdependent mechanism and cell cycle arrest. Am J Physiol Cell Physiol 2018; 315: C28-C43.
- [17] van der Laan M, Horvath SE and Pfanner N. Mitochondrial contact site and cristae organizing system. Curr Opin Cell Biol 2016; 41: 33-42.
- [18] Tombo N, Imam Aliagan AD, Feng Y, Singh H and Bopassa JC. Cardiac ischemia/reperfusion stress reduces inner mitochondrial membrane protein (Mitofilin) levels during early reperfusion. Free Radic Biol Med 2020; 158: 181-194.
- [19] Feng Y, Imam Aliagan A, Tombo N, Draeger D and Bopassa JC. RIP3 translocation into mitochondria promotes mitofilin degradation to increase inflammation and kidney injury after renal ischemia-reperfusion. Cells 2022; 11: 1894.
- [20] Imam Aliagan AD, Ahwazi MD, Tombo N, Feng Y and Bopassa JC. Parkin interacts with Mitofilin to increase dopaminergic neuron death in response to Parkinson's disease-related stressors. Am J Transl Res 2020; 12: 7542-7564.
- [21] Ikeda H, Muroi M, Kondoh Y, Ishikawa S, Kakeya H, Osada H and Imoto M. Miclxin, a novel MIC60 inhibitor, induces apoptosis via mitochondrial stress in beta-catenin mutant tumor cells. ACS Chem Biol 2020; 15: 2195-2204.
- [22] Elefantova K, Lakatos B, Kubickova J, Sulova Z and Breier A. Detection of the mitochondrial membrane potential by the cationic Dye JC-1 in L1210 cells with massive overexpression of the plasma membrane ABCB1 drug transporter. Int J Mol Sci 2018; 19: 1985.
- [23] Feng Y, Madungwe NB, da Cruz Junho CV and Bopassa JC. Activation of G protein-coupled oestrogen receptor 1 at the onset of reperfusion protects the myocardium against ischemia/reperfusion injury by reducing mitochondrial dysfunction and mitophagy. Br J Pharmacol 2017; 174: 4329-4344.
- [24] Kubli DA and Gustafsson AB. Mitochondria and mitophagy: the yin and yang of cell death control. Circ Res 2012; 111: 1208-1221.

# Miclxin-induced Mic60 dysfunction facilitates cell death

- [25] El-Hattab AW, Suleiman J, Almannai M and Scaglia F. Mitochondrial dynamics: biological roles, molecular machinery, and related diseases. Mol Genet Metab 2018; 125: 315-321.
- [26] El-Hattab AW and Scaglia F. Mitochondrial cytopathies. Cell Calcium 2016; 60: 199-206.
- [27] Van Laar VS, Otero PA, Hastings TG and Berman SB. Potential role of Mic60/Mitofilin in Parkinson's disease. Front Neurosci 2018; 12: 898.
- [28] Feng Y, Madungwe NB and Bopassa JC. Mitochondrial inner membrane protein, Mic60/Mitofilin in mammalian organ protection. J Cell Physiol 2019; 234: 3383-3393.
- [29] von der Malsburg K, Müller JM, Bohnert M, Oeljeklaus S, Kwiatkowska P, Becker T, Loniewska-Lwowska A, Wiese S, Rao S, Milenkovic D, Hutu DP, Zerbes RM, Schulze-Specking A, Meyer HE, Martinou JC, Rospert S, Rehling P, Meisinger C, Veenhuis M, Warscheid B, van der Klei IJ, Pfanner N, Chacinska A and van der Laan M. Dual role of Mitofilin in mitochondrial membrane organization and protein biogenesis. Dev Cell 2011; 21: 694-707.

- [30] Takagi H, Matsui Y and Sadoshima J. The role of autophagy in mediating cell survival and death during ischemia and reperfusion in the heart. Antioxid Redox Signal 2007; 9: 1373-1381
- [31] Elmore SP, Qian T, Grissom SF and Lemasters JJ. The mitochondrial permeability transition initiates autophagy in rat hepatocytes. FASEB J 2001; 15: 2286-2287.